Proceedings of the 9th International Conference on Civil Structural and Transportation Engineering (ICCSTE 2024)
Chestnut Conference Centre - University of Toronto, Toronto, Canada – June 13-15, 2024
Paper No. 216
DOI: 10.11159/iccste24.216

Finite Element Modelling of Shear Critical Concrete Beams Reinforced with Basalt Fibres and Basalt Bars

Shahrukh Shoaib[1], Tamer El-Maaddawy[1], Hilal El-Hassan[1], Bilal El-Ariss[1]
[1] United Arab Emirates University
Al Ain P.O. Box 15551, United Arab Emirates
shahrukh.shoaib@uaeu.ac.ae; tamer.maaddawy@uaeu.ac.ae; helhassan@uaeu.ac.ae; bilal.elariss@uaeu.ac.ae

Abstract **-** Finite element (FE) models capable of simulating the nonlinear shear behaviour of concrete beams reinforced with basalt fibres (BF) and basalt fibre-reinforced polymer (BFRP) bars were developed. Experimental tests were carried out to verify the validity of the prediction of the FE models. A parametric study was then conducted to investigate the effectiveness of using BF at different volume fractions (v_f) to upgrade the shear capacity of BFRP-reinforced concrete beams made with recycled concrete aggregates (RCA) with different replacement percentages. Published characterization test results were used as input data in the FE modelling. Results of the FE analysis indicated that beam models with RCA replacement percentages of 30-100% exhibited 10-28% reductions in the shear capacity compared with that of a control beam model made with natural aggregates (NA). The beam models with 30 and 60% RCA containing BF at v_f = 0.5% exhibited a shear capacity comparable to or higher than that of the control beam model with NA. Despite the improvement in the shear response of the beam models with 100% RCA caused by the addition of BF, their shear capacity was lower than that of the control beam model with NA. The shear capacity of the beam model with 100% RCA containing BF at v_f = 1.5% was 93% of that of the control beam model with NA.

Keywords**:** Basalt, concrete, fibres, modelling, recycled aggregates, shear.

1. Introduction

Nonmetallic fibres (BF) have a potential to improve the tensile properties of concrete [1–7]. The addition of BF at v_f = 1.5% to BFRP-reinforced concrete beams with a shear span-to-effective depth ratio (a/d) of 3.3 and 2.5 improved their shear capacity of by 81 and 82%, respectively, relative to those of their counterparts without BF [8]. BFRP-reinforced concrete beams containing BF at v_f of 0.5, 1.0, and 1.33% exhibited 38, 59, and 73% improvements in shear capacity, respectively, relative to that of a control beam without BF [9]. Other published data showed improvement in the shear capacity of 95-98% for BFRP-reinforced concrete beams having BF at v_f = 0.75% and 136-210% for those with v_f = 1.5% [10]. In an effort to preserve natural resources, researchers have explored the potential of replacement of natural aggregates (NA) by recycled concrete aggerates (RC) in the construction industry [11–14]. Although the use of RCA would advance the concept of sustainability and circular economy, concrete mixtures made with RCA exhibit inferior mechanical and durability characteristics [10–12] than those made with NA. BFRP-reinforced concrete beams with RCA percentage replacements of 60 and 100% exhibited 5 and 17% reductions in the shear capacity, respectively, relative to that of a control beam made with NA [15]. The use of 25 and 50% RCA replacement percentage caused 8 and 12% reductions in the shear capacity of concrete beams reinforced with glass fibre-reinforced polymer bars, receptively, relative to that of a control beam made with NA [16].

Information on the shear behaviour of BFRP-reinforced concrete beams containing RCA and BF is scarce in the literature. The shear behaviour of such concrete beams can be examined through analysis of reliable FE models. This study aims to elucidate the interaction between the RCA replacement percentage and the BF volume fraction on the shear response of BFRP-reinforced concrete beams through numerical analysis. Finite element models were developed to simulate the shear behaviour of BFRP-reinforced concrete beams containing BF. Experimental tests were then conducted on BFRP-reinforced concrete beam specimen to verify the validity of the FE models. A parametric study was then conducted to investigate the effect of RCA replacement and inclusion of BF on the shear response of BFRP-reinforced concrete beams. Published characterization test results for concrete mixtures with RCA and BF were used as input data in the FE modelling. Research findings are anticipated to contribute to the widespread use of RCA and BF thus leading to sustainable structures in the built environment.

2. FE Model Development

Two FE models were developed to simulate the shear behaviour of BFRP-reinforced concrete beam containing BF at v_f = 1.0% using the software ATENA [17]. One beam model was made with NA-based concrete, whereas the other one was made with 30% RCA. The beam models had a total length of 2600 mm, width of 150 mm, and depth of 300 mm. The distance between the supports was 2250 mm. The short shear span (test region) had a length of 750 mm, which resulted in a shear span to effective depth ratio (a/d) of the test region of 3. The ratio of the BFRP flexural reinforcement ratio to balanced ratio was (ρ_f/ρ_{fb}) was 2, noting that the value of ρ_{fb} was calculated using based on ACI-440.1R-15 [18]. The tension reinforcement comprised four BFRP bars with a nominal diameter of 10 mm placed at a depth (d) of 250 mm from the compression face. The compression reinforcement consisted of two BFRP bars with a nominal diameter of 6 mm placed at a distance of 30 mm from the compression face of the beam model. The long shear span of the beam models was reinforced with steel stirrups of diameter 8 mm at a spacing of 75 mm to avoid the occurrence of failure outside the test region. Two steel stirrups were provided in the free length outside of the supports to provide adequate anchorage. The concrete and support steel plates were modeled as three-dimensional macro-elements. The BFRP and steel bars were modeled as one-dimensional discrete elements embedded in the concrete macro-element. The mesh size was kept as small as possible at a value of 25 mm. Prescribed vertical displacement was induced at the midpoint of the top surface of the loading steel plate at a rate of 0.1 mm for each step. Restraints were applied as line supports to the middle of the bottom surface of the support plates. The support plate at the end of the test region was restricted from movement in the transverse and vertical directions (y and z directions, respectively). For the support plate outside the test region, restraints were applied in the longitudinal, transverse, and vertical directions (x, y, and z directions, respectively). The numerical values of applied load, deflection, and BFRP strains were recorded using monitoring points. Standard Newton-Raphson iterative solution was adopted in numerical analysis. The details of a typical FE beam model are shown in Fig. 1.

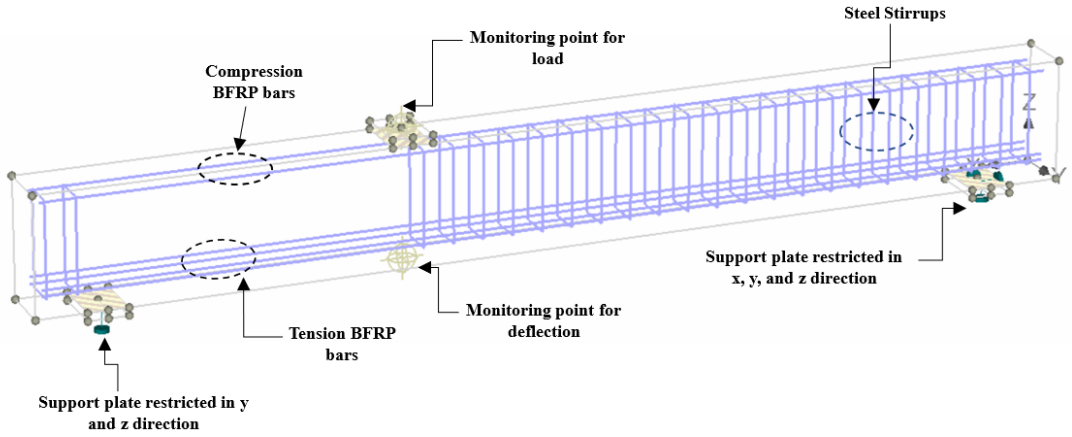

Fig. 1: Details of a typical FE beam model.

The compressive hardening-softening response of concrete mixtures with BF is depicted in Fig. 2a. The compressive plastic response of concrete is represented by multilinear functions. The deviation from linearity initiates at a compressive stress ratio (σ_c/f'_c) of 0.25, where σ_c represents the compressive stress. A significant change in the slope follows at σ_c/f'_c = 0.8 with a respective compressive plastic strain of $0.5\varepsilon_{cp}$, where ε_{cp} refers to the plastic concrete strain at peak. The post-peak plastic compressive stress-strain law descends linearly until a complete release of stress occurs at a plastic strain of ε_d. The tensile softening laws for concrete mixtures with NA and RCA containing BF shown in Fig. 2b,c, respectively, were developed by authors in previously published articles [2,19] based on an inverse analysis of characterization test data. These tensile softening laws were employed as input data in the FE modelling of the present study. A bi-linear stress-strain response

was assumed for the steel stirrups (Fig. 3a). Values of the steel Young's modulus (E_s) and yield strength (f_y) were 200 GPa and 562 MPa, respectively. The stress-strain relationship of the BFRP reinforcing bars was assumed as linear elastic (Fig. 3b), where f_f = stress of BFRP and ε_f = strain of BFRP, f_{fu} = ultimate tensile strength, ε_{fu} = ultimate strain, and E_{frp} is Young's modulus of BFRP. The ultimate tensile strength of the 6- and 10-mm diameter BFRP bars were 904 and 848 MPa, respectively [20]. Their ultimate strain and Young's modulus were 0.02 and 43 GPa, respectively [20]. A perfect bond was assumed between concrete and the reinforcing bars. A previous study implied the adequacy of this assumption to provide an acceptable prediction for the load capacity of concrete elements reinforcement with fibre reinforced polymer bars [21].

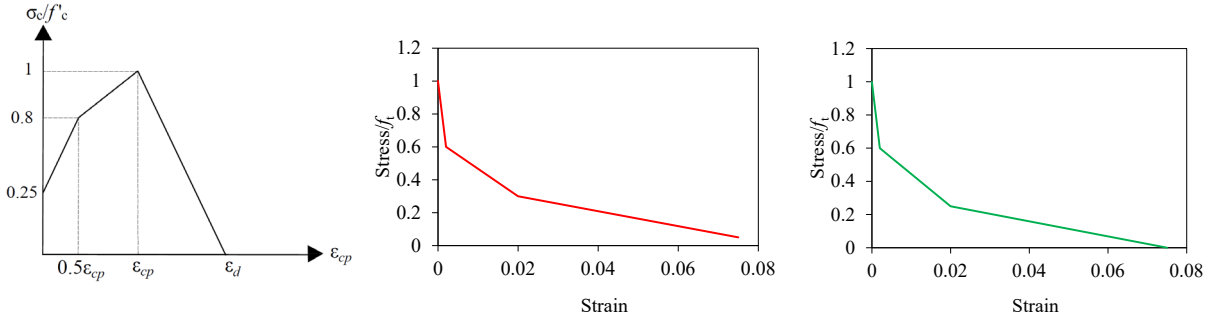

(a) (b) (c)

Fig. 2: Concrete constitutive laws: (a) compressive hardening-softening response; (b) tensile softening response of NA-based concrete; (c) tensile softening response of RCA-based concrete.

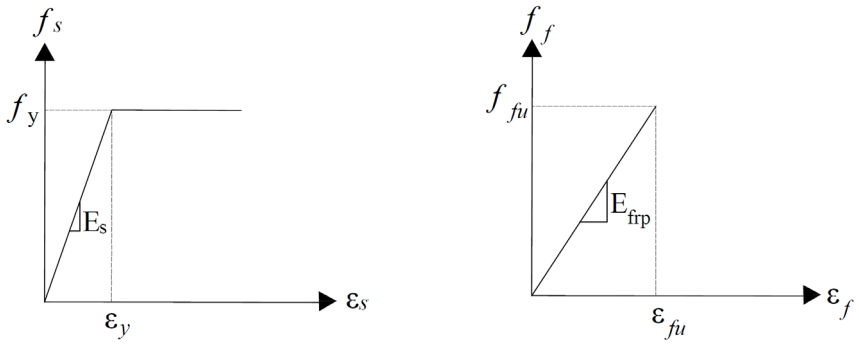

(a) (b)

Fig. 3: Stress-strain relationship of reinforcement: (a) steel; (b) BFRP.

3. Experimental Testing

Two BFRP-reinforced concrete beams were constructed. One beam was made of NA and one beam was made of 30% RCA. Both beams had a hybrid combination of 20- and 50-mm long BF at a ratio of 1:1 to achieve v_f =1%. Key measured concrete properties of the two physical beams are provided in Table 1. The beam specimens are designated as "B-Rx-HB-y" where "B" means beam, "R" denotes RCA, "x" refers to the RCA replacement percentage, "HB" refers to hybrid BF, and "y" refers to the volume fraction of the BF. Photos of BF and BFRP bars used are shown in Fig. 4. A photo showing a beam during testing is provided in Fig. 5. The load was applied at a distance of 750 mm from the center of the left support using a hydraulic actuator. The applied load was measured using a load cell of 500 kN capacity. A linear variable differential transducer (LVDT) was positioned at the lower surface of the beam, aligned with the loading point, to measure deflection. Readings of the load cell and LVDT were collected using a data-logger acquisition system.

Table 1: Mechanical properties of concrete of tested beams.

Specimen	Property			
	f_{cu} (MPa)	f'_c (MPa)	E_c (GPa)	f_r (MPa)
B-R0-HB-1.0	40.0 ± 1.38	28.9 ± 0.75	25.1 ± 1.09	4.50 ± 0.30
B-R30-HB-1.0	35.4 ± 1.70	25.2 ± 2.08	25.4 ± 4.03	4.01 ± 0.38

(a) (b) (c) (d)

Fig. 4: Nonmetallic reinforcement used: (a) 20-mm long BF; (b) 50-mm long BF; (c) 6-mm diameter BFRP bar; (d) 10-mm diameter BFRP bar.

Fig. 5: A physical beam during testing

4. Model Validation

The shear load versus the deflection curves of the beams predicted using FE modelling are compared to those obtained from the experiments in Fig. 6. In alignment with the results of the experimental testing, the FE beam models model exhibited a bi-linear response. The first stage represents the uncracked stage. A deviation from linearity occurred after the initial of flexural cracking. Although, the response of the FE beam models was generally in agreement with that obtained from the experimental tests the post-cracking stiffness of the FE beam beams was slightly higher than that obtained experimentally. Such a minor in the beam stiffness typically occurs in FE modelling because physical concrete beams would typically include shrinkage microcracks that reduce their actual stiffness. Both experimental and numerical results verified that the use of 30% RCA reduced the shear capacity of the beam. The differences between the shear capacity of the FE beam models (V_{FE}) and that measured experimentally ($V_{u,exp}$) were 3 and 16%, respectively, for B-R0-HB-1.0 and B-R30-HB-1.0, respectively.

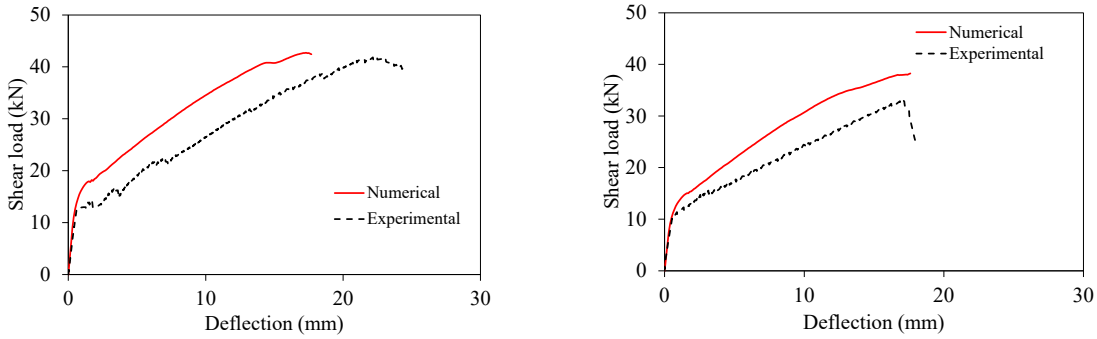

Fig. 6: Shear load-deflection response: (a) B-R0-HB-1.0; (b) B-R30-HB-1.0.

The crack pattern of the FE models at failure is compared to that obtained from the tests Fig. 7. Flexural cracks initiated first at low load values prior to the occurrence of shear cracks. The occurrence of the flexural cracks caused a deviation from linearity as observed in the load-deflection response as shown previously in Fig. 6. As the load increased, a shear crack occurred in the short shear span as planned. Further loads caused an increase in length and width of the critical shear crack initiated in the short shear span. Failure of the beams happened when a complete loss of the shear integrity occurred. This behaviour was predicted using the FE modelling and verified experimentally.

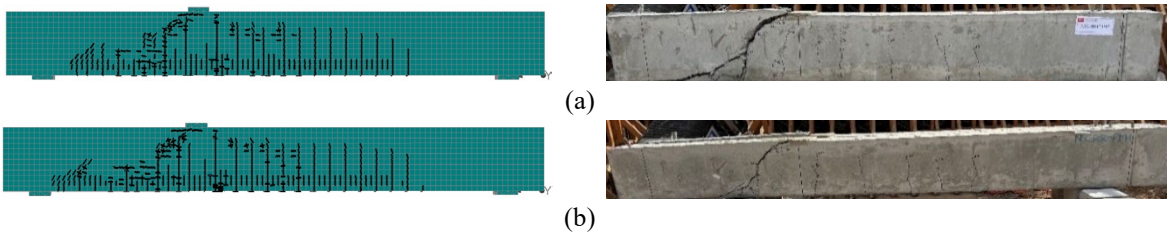

Fig. 7: Cracks pattern at failure: (a) B-R0-HB-1.0; (b) B-R30-HB-1.0.

5. Parametric Study

Additional 13 FE beam models were created to conduct a parametric study aiming at investigating the viability of using BF at different v_f values of 0.5, 1, and 1.5% to improve the shear capacity of BFRP-reinforced concrete beams with different RCA replacement percentages of 30, 60, and 100%. One beam model made with concrete having NA without BF was used as a benchmark. The cylinder compressive strength f'_c value for the control beam model made with NA without BF was taken as 40 MPa. The codified equations proposed by ACI-318-19 [22] were used to determine corresponding values of the concrete Young's modulus (E_c) and concrete rupture strength (f_r) for the control beam model made with NA. The mechanical properties of the concrete mixtures (f_{cu}, f'_c, E_c, and f_t) having different RCA replacement percentages and different BF volume fractions were determined based on regression analysis of published characterization test data [1,2].

Fig. 8 shows the effect of RCA replacement on the shear capacity of the beam models. The beam models with 30, 60, and 100% RCA experience shear strength reductions of 10, 22, and 28%, respectively, compared with that of the control beam model with NA. The reduction in the shear capacity of the beam models with RCA is attributable to the reduced mechanical properties of the concrete with RCA. Fig. 9 illustrates the effect of using BF on the shear capacity of the beam models of the present parametric study. At 30% RCA, adding BF at v_f = 0.5% was sufficient to improve the shear capacity of the beam model with 30% RCA to a level even higher than that of the control beam model with NA (Fig. 9a). The shear capacity of beam model with 30% RCA further increased with increasing the volume fraction of the BF. The FE beam models with 60% RCA and v_f of 0.5% had a shear capacity comparable to that of the control beam model with NA (Fig. 9b). Further

increase in the BF volume fraction resulted in a minor additional increase in the shear capacity of the beam model with 60% RCA. The shear capacities of the FE beam models with 100% RCA and BF were higher than that of their counterparts without BF (Fig. 9c). Nevertheless, their shear capacity was always lower than that of the control beam model with NA. The ratio of the shear capacity of the FE beam model with 100% RCA and v_f of 1.5% to that of the control beam model with NA was 93%.

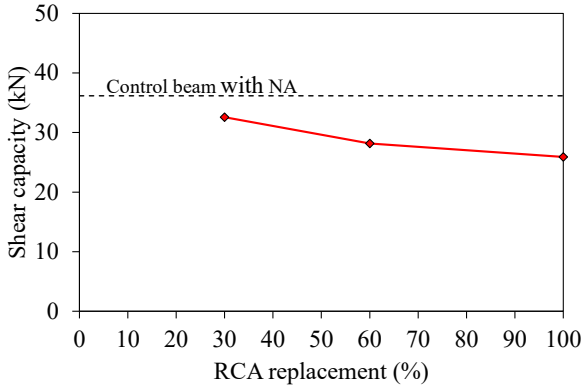

Fig. 8: Effect of RCA replacement percentage on the shear capacity of the beam models.

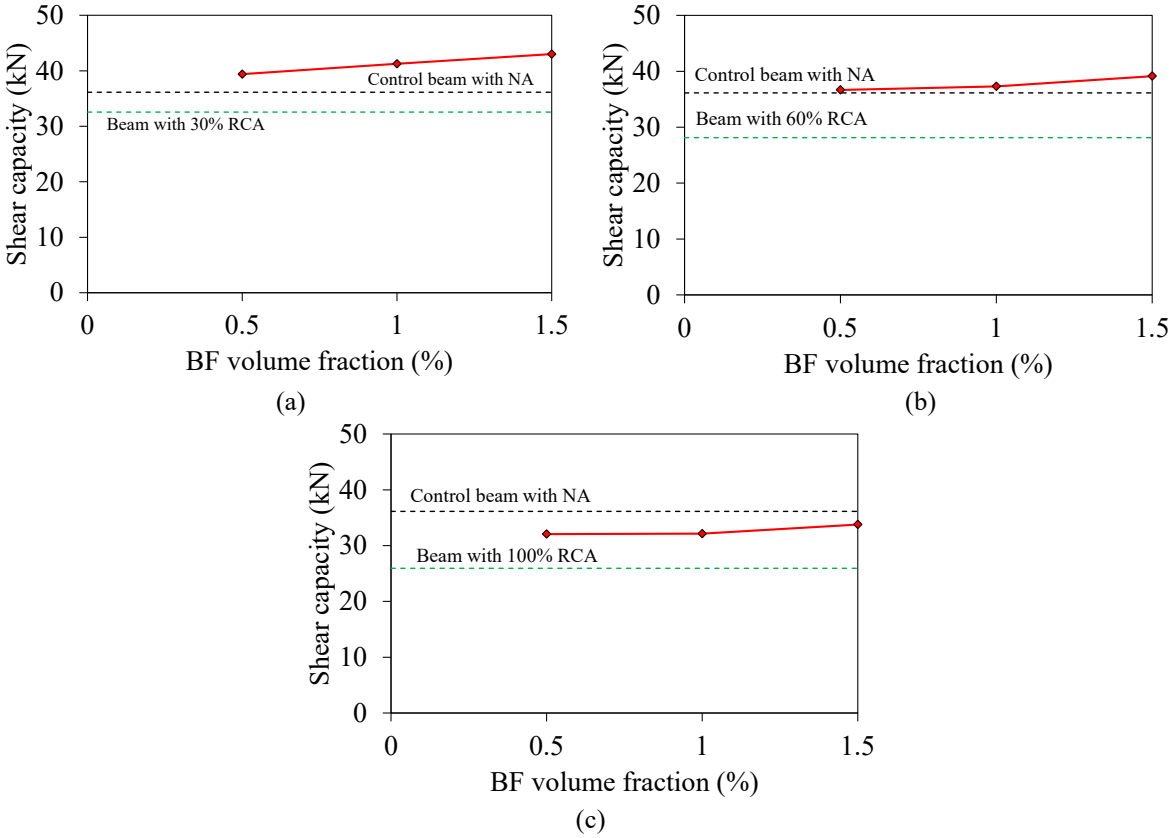

Fig. 9: Effect of BF on the shear capacity of the beam models with RCA: (a) RCA=30%; (b) RCA=60%; (c) RCA=100%.

6. Conclusion

Two FE models were initially developed to simulate the nonlinear shear response of BFRP-reinforced concrete beams containing BF. Predictions of the FE beam models were verified against experimental results of physical concrete beams constructed and tested in the present study. Additional 13 finite element beam models were then developed and employed to carry out a parametric study aimed at investigating the effect of replacement of NA with RCA and the inclusion of BF on the shear capacity of shear critical BFRP-reinforced concrete beams. The main conclusions of the work are summarized herein:

- The FE beam models developed in the present study were able to simulate the shear response, crack pattern, and failure mode of BFRP-reinforced concrete beams containing BF with good accuracy. The difference between the predicted and experimental shear capacities was within a 16% error band. The FE beam models had a slightly higher post-cracking stiffness than that of the actual beams tested in the laboratory.
- The results of the parametric study carried out on FE beam models without BF implied that the shear capacity of BFRP-reinforced concrete beams decreased linearly with an increase in the RCA replacement percentages. BFRP-beam models with 30-100% RCA without BF exhibited 10-28% reductions in their shear capacity relative to that of a control beam model made with NA.
- The results of the FE modelling showed that the addition of BF at v_f = 0.5% to the beam models with 30 and 60% RCA was sufficient to fully restore the shear capacity of the control beam model with NA.
- The FE analysis revealed that the shear capacity of the of FE beam models with 100% RCA and BF was always lower than that of the control beam model with NA irrespective of the content of the BF. The ratio of the shear capacity of the FE beam model with 100% RCA to that of the control beam model with NA was a maximum at a value of 93% when BF was used at v_f of 1.5%.

Acknowledgements

This project is supported by United Arab Emirates University (UAEU) [grant number 12N110].

References

[1] Shoaib S, El-Maaddawy T, El-Hassan H, El-Ariss B, Alsalami M. Characteristics of Basalt Macro-Fiber Reinforced Recycled Aggregate Concrete. Sustainability 2022;14:14267. https://doi.org/10.3390/su142114267.

[2] Shoaib S, El-Hassan H, El-Maaddawy T. Properties and Tensile Softening Laws of Hybrid Basalt Fiber Reinforced Recycled Aggregate Concrete. Buildings 2023;13:975. https://doi.org/10.3390/buildings13040975.

[3] Lee S. Effect of Nylon Fiber Addition on the Performance of Recycled Aggregate Concrete. Appl Sci 2019;9:767. https://doi.org/10.3390/app9040767.

[4] Fang S-E, Hong H-S, Zhang P-H. Mechanical Property Tests and Strength Formulas of Basalt Fiber Reinforced Recycled Aggregate Concrete. Materials 2018;11. https://doi.org/10.3390/ma11101851.

[5] Wang Y, Hughes P, Niu H, Fan Y. A new method to improve the properties of recycled aggregate concrete: Composite addition of basalt fiber and nano-silica. J Clean Prod 2019;236:117602. https://doi.org/10.1016/j.jclepro.2019.07.077.

[6] Ali B, Qureshi LA, Raza A, Nawaz MA, Rehman SU, Rashid MU. Influence of Glass Fibers on Mechanical Properties of Concrete with Recycled Coarse Aggregates. Civ Eng J 2019;5:1007–19. https://doi.org/10.28991/cej-2019-03091307.

[7] Meesala CR. Influence of different types of fiber on the properties of recycled aggregate concrete. Struct Concr 2019;20:1656–69. https://doi.org/10.1002/suco.201900052.

[8] El Refai A, Alnahhal W, Al-Hamrani A, Hamed S. Shear performance of basalt fiber-reinforced concrete beams reinforced with BFRP bars. Compos Struct 2022;288:115443. https://doi.org/10.1016/j.compstruct.2022.115443.

[9] Mohaghegh AM, Silfwerbrand J, Årskog V. Shear behavior of high-performance basalt fiber concrete—Part I: Laboratory shear tests on beams with macro fibers and bars. Struct Concr 2018;19:246–54. https://doi.org/10.1002/suco.201700208.
[10] Muhammad JH, Yousif AR. Effect of basalt minibars on the shear strength of BFRP-reinforced high-strength concrete beams. Case Stud Constr Mater 2023;18:e02020. https://doi.org/10.1016/j.cscm.2023.e02020.
[11] Rahal K. Mechanical properties of concrete with recycled coarse aggregate. Build Environ 2007;42:407–15. https://doi.org/10.1016/j.buildenv.2005.07.033.
[12] Kou S-C, Poon C-S. Long-term mechanical and durability properties of recycled aggregate concrete prepared with the incorporation of fly ash. Cem Concr Compos 2013;37:12–9. https://doi.org/10.1016/j.cemconcomp.2012.12.011.
[13] Chakradhara Rao M, Bhattacharyya SK, Barai SV. Influence of field recycled coarse aggregate on properties of concrete. Mater Struct 2011;44:205–20. https://doi.org/10.1617/s11527-010-9620-x.
[14] Fonseca N, de Brito J, Evangelista L. The influence of curing conditions on the mechanical performance of concrete made with recycled concrete waste. Cem Concr Compos 2011;33:637–43. https://doi.org/10.1016/j.cemconcomp.2011.04.002.
[15] Shoaib S, El-Maaddawy T, El-Hassan H, El-Ariss B. Behavior of Shear-Critical Recycled Aggregate Concrete Beams Containing BFRP Reinforcement. Buildings 2023;13:2785. https://doi.org/10.3390/buildings13112785.
[16] Karimi Pour A, Shirkhani A, Zeng J-J, Zhuge Y, Noroozinejad Farsangi E. Experimental investigation of GFRP-RC beams with Polypropylene fibers and waste granite recycled aggregate. Structures 2023;50:1021–34. https://doi.org/10.1016/j.istruc.2023.02.068.
[17] ATENA | Cervenka Consulting n.d. https://www.cervenka.cz/products/atena/ (accessed June 21, 2022).
[18] ACI 440.1R-15; Guide for Design and Construction of Structural Concrete Reinforced with Fiber-Reinforced Polymer (FRP) Bars, American Concrete Institute: Farmington Hills, MI, USA, 2015.
[19] Shoaib S, El-Hassan H, El-Maaddawy T. Performance Evaluation and Development of Tensile Softening Law for Concrete Reinforced with Different Sizes and Combinations of Basalt Fibers. J Mater Res Technol 2023. https://doi.org/10.1016/j.jmrt.2023.05.095.
[20] Reforcetech n.d. https://reforcetech.com/ (accessed December 3, 2020).
[21] Gooranorimi O, Claure G, Suaris W, Nanni A. Bond-slip effect in flexural behavior of GFRP RC slabs. Compos Struct 2018;193:80–6.
[22] ACI-318-19(22); Building Code Requirements for Structural Concrete and Commentary (Reapproved 2022). American Concrete Institute: Farmington Hills, MI, USA, 2022.